Biochimie 140 (2017) 58–65

Contents lists available at ScienceDirect

Biochimie

journal homepage: www.elsevier.com/locate/biochi

Research paper

Contribution of the carbohydrate-binding ability of *Vatairea guianensis* lectin to induce edematogenic activity

Gabriela F.O. Marques [a, 1], Vinicius J.S. Osterne [b, 1], Livia M. Almeida [a], Messias V. Oliveira [b, 2], Luiz A.C. Brizeno [a], Vanir R. Pinto-Junior [b], Mayara Q. Santiago [b], Antonio H.B. Neco [b], Mario R.L. Mota [c], Luiz A.G. Souza [d], Kyria S. Nascimento [b], Alana F. Pires [a], Benildo S. Cavada [b, *], Ana M.S. Assreuy [a, **]

[a] Institute of Biomedical Sciences, State University of Ceará, Av. Paranjana, 1700, 60740-000, Fortaleza, CE, Brazil
[b] Department of Biochemistry and Molecular Biology, Federal University of Ceará, Mr. Hull s/n Building 907, 60445-970, Fortaleza, CE, Brazil
[c] Department of Dental Clinic, Division of Oral Pathology, Federal University of Ceará, R. Alexandre Baraúna, 949, 60430-160, Fortaleza, CE, Brazil
[d] Instituto Nacional de Pesquisas da Amazônia - INPA, Manaus, Amazonas, Brazil

ARTICLE INFO

Article history:
Received 23 March 2017
Accepted 9 June 2017
Available online 16 June 2017

Keywords:
Vatairea guianensis
Lectin
Molecular modeling
Molecular docking
Inflammation

ABSTRACT

Vatairea guianensis lectin (VGL), Dalbergiae tribe, is a N-acetyl-galactosamine (GalNAc)/Galactose (Gal) lectin previously purified and characterized. In this work, we report its structural features, obtained from bioinformatics tools, and its inflammatory effect, obtained from a rat paw edema model. The VGL model was obtained by homology with the lectin of *Vatairea macrocarpa* (VML) as template, and we used it to demonstrate the common characteristics of legume lectins, such as the jellyroll motif and presence of a metal-binding site in the vicinity of the carbohydrate-recognition domain (CRD). Protein-ligand docking revealed favorable interactions with *N*-acetyl-D-galactosamine, D-galactose and related sugars as well as several biologically relevant *N*- and *O*-glycans. *In vivo* testing of paw edema revealed that VGL induces edematogenic effect involving prostaglandins, interleukins and VGL CRD. Taken together, these data corroborate with previous reports showing that VGL interacts with *N*- and/or *O*-glycans of molecular targets, particularly in those presenting galactosides in their structure, contributing to the lectin inflammatory effect.

1. Introduction

Widely distributed among living organisms and viruses, lectins are proteins or glycoproteins capable of forming complexes with molecules and biological structures containing saccharides [1]. Since lectins can reversibly bind to carbohydrates, these molecules play major roles in cell communication, such as that occurring in the inflammatory process via glycocode decoding in the structure of soluble and integral cell membrane glycoconjugates [2].

Among lectins, those purified from leguminous plants are widely studied. This group comprises a large family of closely related lectins with similarity in physicochemical and structural properties, but significant differences in their biological activities [3]. Some lectins of the Dalbergieae tribe (Fabaceae, Papilionoideae) have now been purified and characterized. Moreover, the structures of *Pterocarpus angolensis* [4], *Centrolobium tomentosum* [5], *Platypodium elegans* [6], *Arachis hypogaea* [7] and *Vatairea macrocarpa* [8,9] lectins have already been solved. Those lectins possessing binding affinity for *N*-acetyl-glucosamine present anti-inflammatory property, such as the lectin of *Lonchocarpus sericeus* [10–12] and *Lonchocarpus araripensis* [13]. However, those lectins with binding affinity for galactose, such as *Vatairea macrocarpa* lectin, present inflammatory property [14–16]. In addition, the inflammatory effect of *V. macrocarpa* lectin occurs via activation of macrophages with release of cytokines [16].

The *N*-acetyl-D-galactosamine/D-galactose-specific lectin of *Vatairea guianensis* (VGL) is a homotetrameric glycoprotein with

* Corresponding author.
** Corresponding author.
E-mail addresses: messiassigma@gmail.com (M.V. Oliveira), bscavada@ufc.br (B.S. Cavada), anassreuy@gmail.com (A.M.S. Assreuy).
[1] Equal contribution.
[2] Participated in the new docking experiments and in paper writing.

http://dx.doi.org/10.1016/j.biochi.2017.06.008
0300-9084/

two *N*-glycosylations at Asn111 and Asn183. It was purified by affinity chromatography and possesses a molecular mass of 120 kDa. VGL presents *in vitro* vasodilator effect, inducing relaxation in endothelialized aorta via nitric oxide [17]. We aimed to gain a better understanding of VGL-saccharide binding (CRD) in the context of VGL biological effects. To accomplish this, we modeled the three-dimensional structure of VGL and focused on its *in vivo* vasodilator effects on a rat paw edema model.

2. Materials and methods

2.1. Lectin isolation

VGL was isolated from *Vatairea guianensis* seeds by ion exchange chromatography (DEAE-Sephacel column), followed by affinity chromatography (guar gum) [17]. The pure protein was diluted in sterile saline (0.9% NaCl) before biological assays.

2.2. Rat paw edema model

VGL (0.01, 0.1 and 1 mg/kg) was administered by subcutaneous (s.c.) route in Wistar rats (150–200 g) as inflammatory stimulus. Controls received sterile saline (0.1 mL/100 g body mass). The experimental protocols were approved by our Institutional Ethical Committee (UECE No. 10130208-8/40).

Paw edema was measured by hydroplethysmometry immediately before VGL injection (zero time), and from 0.5 to 72 h thereafter and was expressed as the variation in paw volume (mL) or area under curve (arbitrary units) [18] compared to zero time.

The participation of inflammatory mediators in the lectin effect was evaluated by treating the animals with the following pharmacological inhibitors: nitric oxide synthase (N-Nitro-L-arginine methyl ester/L-NAME; 25 mg/kg; intravenous), cyclooxygenase (indomethacin; 5 mg/kg; subcutaneous) andinterleukin-1β (thalidomide; 45 mg/kg; intraperitoneal) [19] 30 min before VGL administration (1 mg/Kg; s.c.).

The participation of the lectin carbohydrate-recognition domain (CRD) was evaluated by the injection of the most active dose of VGL (1 mg/kg) after incubation (30 min/37 °C) with its binding sugar galactose (0.1 M). Galactose was individually incubated at the same conditions as control.

2.3. Histological analysis

Paw tissues were removed 6 h after VGL (1 mg/kg) administration, fixed with 10% buffered formalin for 24 h, embedded in paraffin, cut into 5-μm thick slices, stained with hematoxylin & eosin (HE) and analyzed by light microscopy coupled to image acquisition systems (ScopePhoto; Image Manager 50). The intensity of tissue inflammation was graded according to the following scores: 0. normal tissue (no distinguishable change, 0%), absence of inflammatory infiltrate; 1. discrete tissue changes (initiation of changes, up to 30%), slight inflammatory infiltrate; 2. moderate tissue changes (patent changes, 31–60%), moderate inflammatory infiltrate; and 3. severe tissue changes (widespread changes, 61–100%), severe inflammatory infiltrate.

2.4. Immunohistochemistry

Fragments of paw tissue were sectioned to a thickness of 3 μm, placed on silanized slides and processed as described in the following protocol. Samples were deparaffinized, subjected to rehydration and antigen-recovery using citrate buffer (pH 6.0), incubated (10 min; r.t.) with 6% H_2O_2 in methanol (1:1) and washed with TRIS pH 7.6 (TRIS) in order to inactivate endogenous peroxidases. Samples were re-incubated for 1 h (r.t.) with the primary antibody (Ab) against IL-1β (monoclonal; Abcam "AB9787"; 1:100), washed and further incubated (30 min; r. t.) with biotinylated immunoglobulin (Ig; DAKO E0468) and streptavidin (DAKO P0397). Diaminobenzidine chromogen (DAKO K3469) was applied for 10 min, and Mayer's hematoxylin was used for counterstaining. Samples were dehydrated (ethanol and xylene) and cover-slipped with permanent Mounting medium. Parallel sections were treated with control IgG instead of the primary Ab.

For semi quantitative immunohistochemical evaluation, sections were randomly selected in 5 fields (400x magnification) in areas of greater concentration of immunostained cells located in connective or epithelial tissue. The percentage of cells with cytoplasmic or nuclear expression was scored as follows: (0) no positive cells; (1 - mild) 1–33% positive cells; (2 - moderate) 34–66% positive cells; (3 - intense) 67–100% positive cells (adapted from Minal Chaudhary et al. 2012) [20].

2.5. Statistical analysis

The *in vivo* data were presented as mean ± SEM, and the statistical analysis was performed by ANOVA, followed by Bonferroni's test. P values < 0.05 were considered significant. Histopathological and immunohistochemical data were expressed as median (maximum and minimum) and analyzed by Mann-Whitney test.

2.6. Template determination and secondary structure prediction

VGL sequence was downloaded from the Universal Protein Resource (Uniprot) (ID: P86893). The template for homology modeling was obtained from BLASTp search on the Protein Data Bank (PDB) with default parameters. Proteins most similar to VGL were chosen and ranked based on their resolution and geometric parameters.

Secondary structure prediction was carried out using PsiPro server, an automated system for secondary structure prediction [21]. The secondary structure was applied as one of the validation factors for homology model selection.

2.7. Homology modeling and validation

The 3D structure of VML in complex with Tn antigen (PDB ID: 4U36) was downloaded from PDB as the template structure. The homology model of VGL was built with MODELLER v.9.16 [22]. VGL and VML structures were aligned using salign module, followed by manual optimization. Initially, a hundred models were generated and ranked based on the Modeller objective score function (molpdf) and Discrete Optimized Protein Energy (DOPE) scores. Several models with lower molpdf and DOPE were selected and submitted to validation of stereochemical properties like Ramachandran plot, steric overlaps, Cβ deviation parameters, rotamers, and bond angle deviations using PROCHECK [23]. Side-chain acceptability was obtained by the Verify3D server [24]. QMEAN and Z-scores were also assessed by Protein Structure and Assessment tools [25–27]. The model having the best values in all validations was selected and applied in the subsequent analyses. Molecular drawings were prepared with PyMol (Shrodinger, LLC).

2.8. Molecular docking

Molecular docking was applied to verify the VGL ability to interact with several sugars. In order to perform the dockings, energy minimized saccharides structures were downloaded from PubChem [28]. Simulations were carried out with CLC Drug Discovery Workbench (CLC Bio; Boston, MA, USA), a software that uses

a standard precision mode to determine the favorable binding poses and detect several flexible ligand conformations, while holding the protein as a rigid structure. The location of VGL CRD was obtained by superposition with VML using. As docking parameters, the binding radius set to 10 $Å^3$ around VGL CRD and the number of iterations set to 5000. The PLANTSPLP algorithm was applied to calculate docking score [29], where more negative values indicate stronger interaction, and the best poses for each ligand were selected based on hydrogen bonds and hydrophobic interactions. LIGPLOT+ [30] and PyMol were applied to generate the 2D interaction plots and molecular representations, respectively. The result for GalNAc pose was compared to that in the VML crystal structure (PDB ID: 4U2A).

2.9. N- and O-glycans docking

VGL structure was also submitted to molecular docking with several *N*- and *O*-glycans commonly found in glycoproteins. Glycans structures were obtained from several scientific works [31–33] and built with the carbohydrate builder tool of GlycamWeb [34] All glycans were submitted to energy minimizations using AMBER 12 [35] with GLYCAM_06j-1 force field [36] via GlycamWeb built in modules. Missing hydrogen atoms and bond type corrections were performed by ligand preparation module of Hermes v. 1.8.2. Glycans structures representations are shown in Fig. S1. Docking simulations were performed with GOLD v. 5.5 (Genetic Optimization for Ligand Docking – CCDC, Cambridge, England). GOLD implements a generic algorithm to dock ligands into protein binding sites exploring a great range of ligands conformations with partial protein flexibility [37]. VGL was prepared for docking by removal of solvent and ligand molecules. Binding site was defined in center of carbohydrate-recognition domain and all atoms comprising 12 Å of radius. Docking parameters were: population size of 100, selection pressure of 1.1, number of operations of 10,000, number of islands of 5, niche size of 2 and crossover frequency of 95. For all ligands, 20 poses were generated and filtered by docking score, oligosaccharide geometry, hydrogen bonds and hydrophobic interactions coherence. Further validation was performed by comparing interactions with those from VGL-Galactose complex and removing poses with serious geometric strains. PLANTSPLP was chosen as score function [29] and VGL-Galactose score was used as comparison. All other options were program default. VGL-glycans complexes figures were generated in PyMol.

3. Results and discussion

VGL induced a time- and dose-dependent paw edema that lasted 48 h (Fig. 1a) at 0.01 mg/Kg (0.21 ± 0.03 AUC); 0.1 mg/Kg (0.42 ± 0.06 AUC) and 1 mg/Kg (0.59 ± 0.08 AUC) compared to saline (0.06 ± 0.02 AUC) (Fig. 1b). At 1 mg/Kg, VGL showed maximal efficacy (4–8 h), initiating edematogenic effect 30 min after administration (Fig. 1a). VGL at 1 mg/Kg also induced polymorphonuclear infiltrate along the edema time-course, which was accentuated at 6 h [VGL: median 3 (3.3)*; p = 0.0022 *vs.* saline: median 0 (0.1)] (Fig. 2). These results corroborate the typical acute inflammatory process demonstrated by the macroscopic evaluation shown in Fig. 1 and are in accordance with previous studies performed with the homologous lectin VML that elicited acute edematogenic activity accompanied with leukocyte infiltration [15].

Pharmacological modulation, as performed by treating animals with inhibitors of inflammatory mediators before VGL injection, implied the participation of prostaglandins in the *in vivo* vasodilator effect (edema) of VGL since indomethacin (inhibitor of the enzyme cyclooxygenase that catalyzes the synthesis of prostaglandins caused moderate (37%) inhibitory effect. In contrast, L-NAME (inhibitor of the enzyme NOS that catalyzes the synthesis of NO) did not modify the lectin edematogenic effect, despite the important vasodilator effect of NO. These data seem to contradict the vasodilator effect of VGL as previously shown *in vitro* [17]. However, this could be explained by the different NOS isoforms expressed in the noninflamed vessels (endothelial NOS) and the vessels in inflamed paw tissues (inducible NOS) [38]. In addition to the implication of prostaglandins, also a vasodilator mediator, we demonstrated an important participation of interleukins since thalidomide inhibited the edema induced by VGL by 62% (Fig. 3).Corroborating the results obtained by pharmacological modulation, IL-1β immunostaining was revealed at 6 h in the epithelial and connective tissues (fibroblasts and inflammatory cells): epithelium [saline: 2 (1.2) *vs.* VGL: 3 (2.3)*]; connective tissue [saline: 0 (0.1)*vs.* VGL: 3 (2.3)*] (Fig. 4). These data are in line with the role of prostaglandins and IL-1β, both mediators of cellular origin, in acute inflammation inducing vasodilatation and tissue damage [39], as well as the demonstrated effect of VML on acute models of inflammation with the participation of prostaglandins

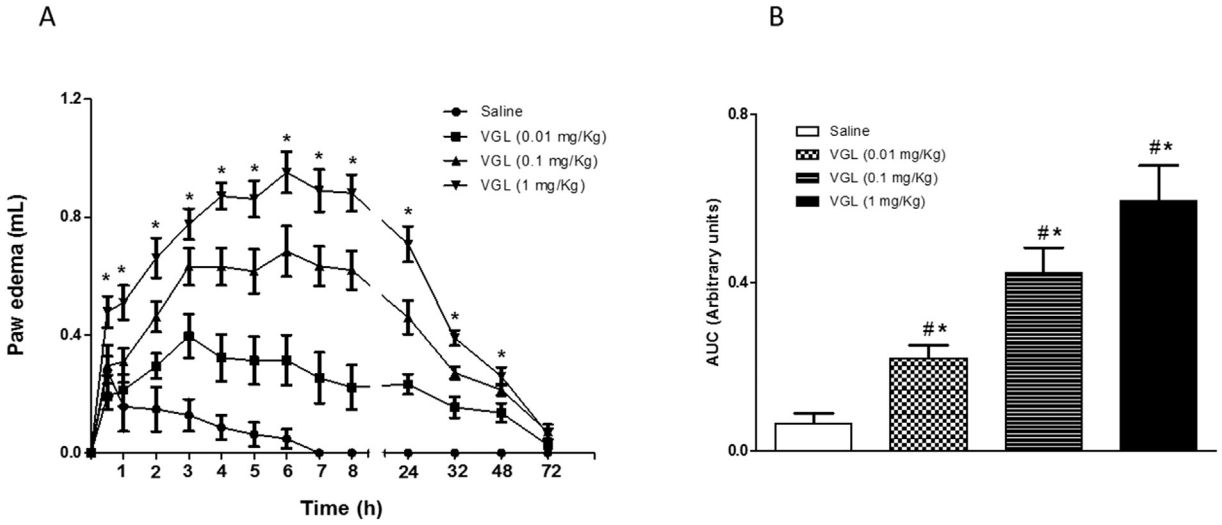

Fig. 1. VGL induces dose- and time-dependent paw edema. VGL (0.01, 0.1, 1 mg/kg; s.c.) or saline was injected intraplantar, and edema was measured before (zero time) and from 0.5 to 72 h after VGL. (a) Time course and (b) area under curve (AUC). Mean ± S.E.M. (n = 5–6). *p < 0.05 *vs.* saline; #p < 0.05 *vs.* VGL at all doses.

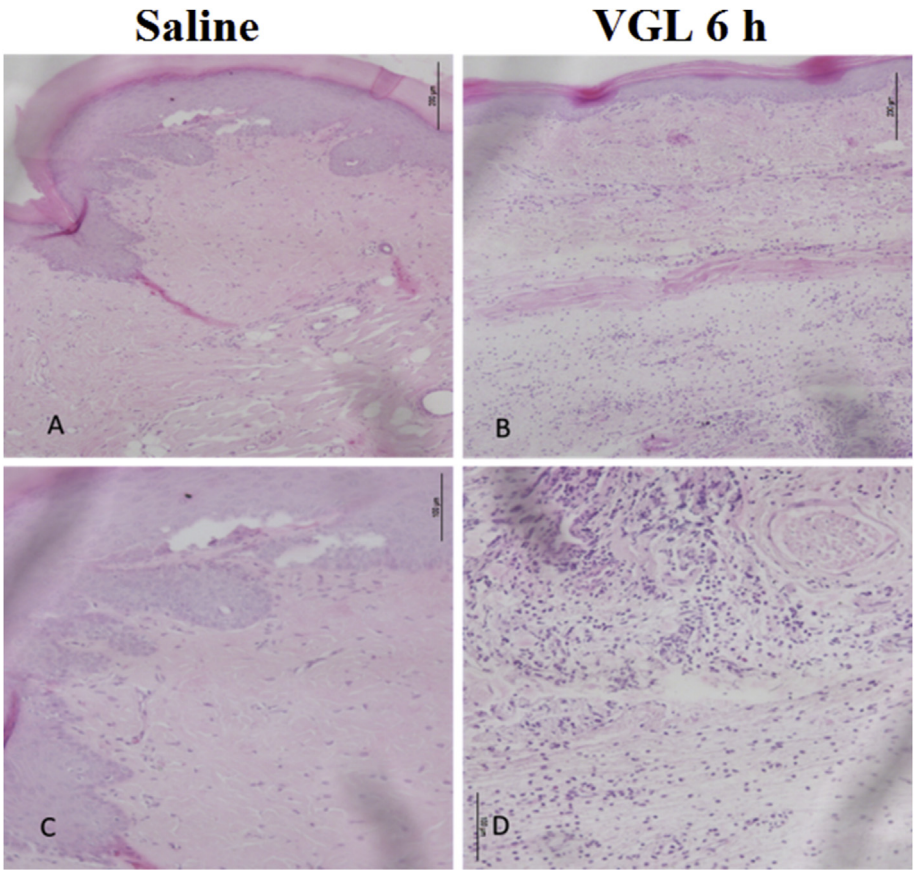

Fig. 2. VGL induces paw edema with polymorphonuclear leukocyte infiltrate. VGL (1 mg/kg; s.c.) or saline was injected intraplantar, and histological analysis was performed at 6 h. (a,c) Saline, (b,d) VGL.

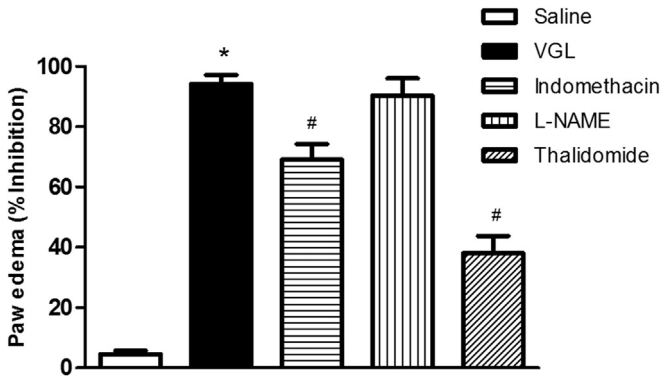

Fig. 3. The paw edema induced by VGL involves prostaglandins and interleukins. VGL (1 mg/kg; s.c.) was injected in the paw of naïve or treated animals 30 min before indomethacin (5 mg/kg, s.c.), L-NAME (30 mg/kg; i.v.) or thalidomide (45 mg/kg; i.p.). Mean ± S.E.M. (n = 5–6). *p < 0.05 *vs.* saline; #p < 0.05 *vs.* VGL.

and interleukins [15].

Importantly, classical literature has implicated the participation of the carbohydrate-recognition domain (CRD) in the inflammatory effects of leguminous lectins isolated from the tribes Phaseoleae [32,33] and Dalbergieae [10,13,15], demonstrated by the partial or total inhibition of the lectin activity by its binding sugar [40].

The protein BLAST analysis of VGL sequence demonstrated 93% identity with VML sequence (4U36) and because of this, VML was chosen as the template for homology modeling of VGL using the MODELLER 9.16 suite. Secondary structure prediction resulted in a prevalence of β-sheet structures and loops with absence of α-helix (Fig. S2).This result agrees with previously reported data for other lectins. VGL monomer is shown in Fig. 5.

Reliability of the VGL model obtained by homology modeling was assessed by various validation parameters. For the chosen model, PROCHECK analysis showed that local and global stereochemical parameters had favorable values. Ramachandran plot indicated that 100% of the residues are in favorable and allowed regions of the graph. The QMEAN global and QMEAN z-score, as obtained by the protein assessment tools, were 0.755 and −0.156, both within the range of high-quality models. Compatibility of the amino acid sequence and three-dimensional structure was obtained by the Verify3D program, in which 92.89% of the residues were compatible, suggesting that the side-chain environment is acceptable. Also, the superposition between the best model and the template resulted in a root mean square deviation (RMSD) of 0.143, indicating reliable prediction. Altogether, these analyses demonstrated that the VGL model was comparable to those of experimental structures, indicating that the modeled structure was adequate for the subsequent tests. VGL monomer was shown to be typical of legume lectin fold, consisting of a β-sandwich presenting the jellyroll motif with an antiparallel β-sheet of six strands partially extended and another curved antiparallel β-sheet of seven strands interconnected by loops of variable length. The monomer presents a single CRD stabilized by two divalent cations: calcium and manganese, both present in the metal bind site (MBS) in the vicinity of CRD.

Tetrameric biological assembly of VGL was experimentally determined by Silva and colleagues [17]. Tetramer is composed of

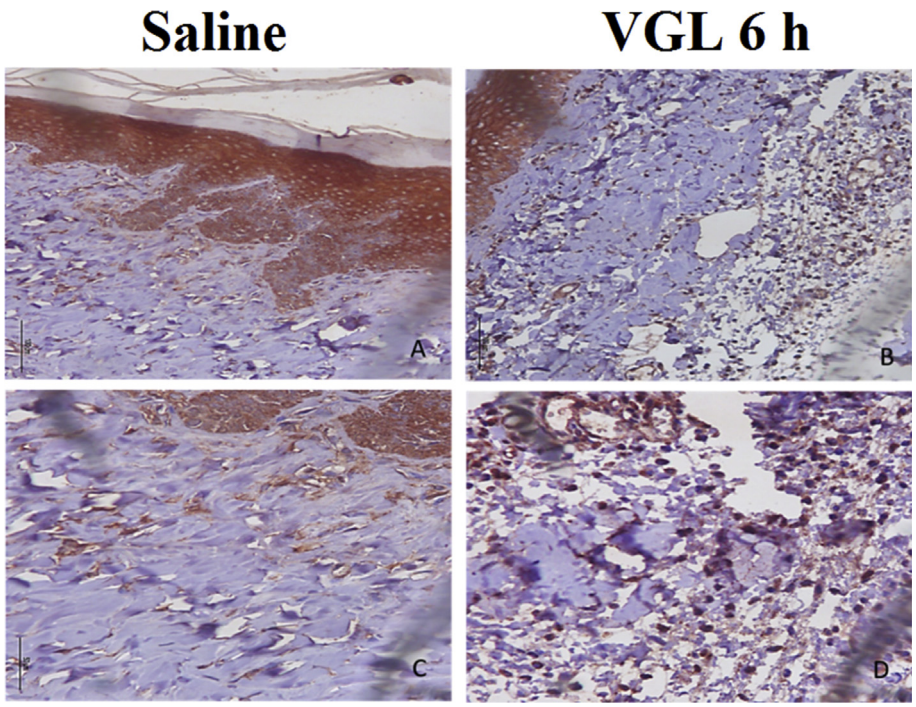

Fig. 4. IL-1β plays an important role in VGL-induced paw edema. VGL (1 mg/kg; s.c.) or saline was injected intraplantar, and immunohistochemistry for IL-1β in epithelial and connective paw tissues fragment was performed at 6 h. (a,c) Saline, (b,d) VGL.

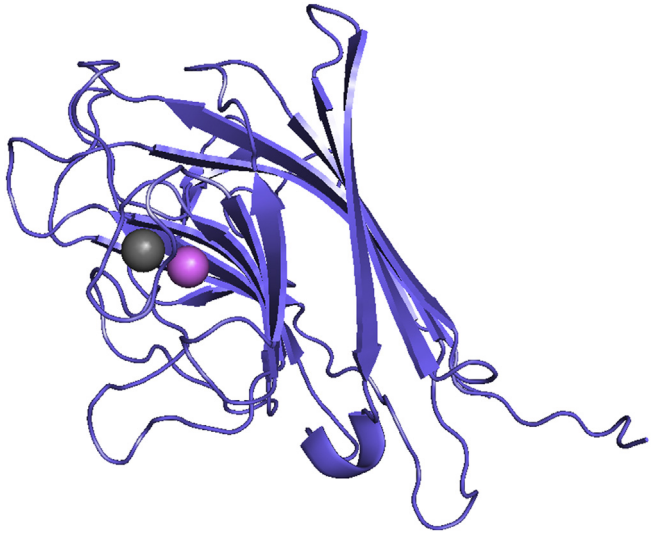

Fig. 5. Overall structure of VGL monomer. VGL chain is shown in cartoon representation colored in blue. Spheres represent calcium ion (in gray) and manganese ion (in purple).

two dimers oppositely arranged to form large central cavity which is, in turn, formed by interactions between the outermost loops of the six-stranded β-sheets of each monomer, generating a type 2 canonical interface. Other lectins, such as VLLB4, PHA and SBA, also present this kind of oligomerization [41].

Similar to VML, CRD and metal binding sites (MBS)are conserved in VGL. Carbohydrate-recognition domain is an exposed region in protein surface formed by four loops (see more details in molecular docking section), and for MBS, calcium ion is coordinated by Phe127, Asp125, Asp132, while the manganese ion is coordinated by Glu123, Asp125, Asp132 and His137 (Fig. S3).

The results demonstrated that VGL presents favorable interactions with GalNAc and D-galactose, corroborating previous inhibition assays [17]. Like other lectins, the binding with sugars is mediated by Van der Waals, hydrophobic and hydrogen interactions [4,5,8].

The results demonstrated that VGL presents favorable interactions with GalNAc (Score: −50.11), Gal (Score: −42.80), α-methyl-D-galactoside (−43.11) and α-Lactose (−43.45) corroborating with previous sugar inhibition assays performed by Silva and colleagues [17]. Comparison of scores and experimental data is shown in Table 1, and indicates the lectin specificity for galactosides.

The set of interactions established between the VGL model and galactose is shown in Fig. 6a. The galactose residue was stabilized by a network of H-bonds and hydrophobic interactions. The amino acid residues Asn87, Asn129, Leu213 and Ser214 interact by H-bonds with oxygen atoms O2, O3, O4 and O6 from carbohydrate structure. Gly104, Phe127, Gly212 and His217 residues are responsible for hydrophobic interactions which stabilize the galactose residue in the CRD. The *N*-acetyl-D-galactosamine residue complexed in the CRD was stabilized by a network of H-bonds connecting Asp87, Gly105, Asn129, Leu213, Ser214 and His217 residues to oxygen atoms O3, O4, O5 and O6 present in the molecule. Hydrophobic interactions involving the amino acid residues Gly104, Phe106, Phe127, Trp131 and Gly212 also contribute to the binding of lectin with this carbohydrate (Fig. 6b). The larger number of interactions with GalNAc in relation to Gal was suggested in previous study [17] and was confirmed here. Previous results demonstrated the strong binding of *Vatairea macrocarpa* lectin (VML) with galactosides [8,9]. As shown in Fig. S4, superposition of VGL with the structure of VML complexed with GalNAc demonstrated remarkable similarity of ligand binding validating the docking experiments.

These results demonstrated the efficiency of homology modeling and molecular docking for VGL. In fact, the animal

Table 1
Docking score results and minimum inhibitory concentration of carbohydrates on VGL hemagglutination activity.

	Score[a]	MIC[b] (mM)[e]
Carbohydrate		
N-acetyl-D-galactosamine	−50.11	1.0
α-methyl-D-galactoside	−43.11	NT[c]
α-Lactose	−43.45	2.0
α-D-galactose	−42.80	8.2
α-D-glucose	−39.26	NI[d]
N-acetyl-D-glucosamine	−39.03	NI
N-acetyl-D-mannosamine	−39.00	NT
α-methyl-D-glucoside	−38.68	NT
Sucrose	−38.01	NI
α-methyl-D-mannoside	−36.87	NT
α -D-mannose	−35.66	NI
α-L-fucose	−34.03	NI
***N*-glycans**		
CMPLX1	−53.65	
CPLX2	−35.03	
HBRD1	9.60	
HBRD2	−52.28	
MAN5	−33.06	
MAN9	−39.03	
***O*-glycans**		
Tn antigen	−52.00	
T antigen	−44.08	
Excore1	−50,85	
Excore2	−53.60	
Excore3	−32.00	
Excore4	−51.14	

[a] Moldock score (MDS) = $E_{inter} + E_{intra}$, where E_{inter} is the ligand protein interaction energy: .
[b] MIC: minimum inhibitory concentration.
[c] NT: not tested.
[d] NI: not inhibitory on tested concentrations.
[e] Data from Silva and colleagues [17].

experiments indicated partial inhibition (40%) of VGL edematogenic effect (0.35 ± 0.05 AUC) in response to the association of VGL and galactose (0.22 ± 0.03 AUC) (Fig. 6c). This partial inhibition could be explained by the involvement of other binding sites on the molecule, such as metal or hydrophobic cavity [42,43]. Alternatively, the lectin would have high affinity for *N*- and *O*-glicans, present in the cell membrane, despite of the high galactose concentration used in the reversion assay. Attempting to confirm VGL capacity of interactions with glycoproteins a total of 13 glycans, 6 *N*- and 7 *O*-glycans, were chosen for docking based primarily on its relevance and relative high presence in glycoproteins. Best docking poses and scores are shown in Fig. S5 and Table 1 respectively. Among *N*-glycans, complex type presenting galactosyl terminal moieties demonstrated favorable interactions with the lectin (CPLX1 score: −53.65) (Fig. 7A) but the addition of a sialic acid moiety reduced the score drastically (CPLX2 Score: −35.03) due to galactosyl capping. Similarly, hybrid *N*-glycans presenting galactose in terminal region interact strongly with VGL (HBRD2 Score: −52.28) differently to that occurs with its sialylated counterpart (HBRD1 Score: 9.60). Unsurprisingly high-mannose type did not show important interactions in CRD.

Sugar sequences found in glycoproteins normally share a common core, in case of *N*-glycans Manα1−6 (Manα1−3)Manβ1−4GlcNAcβ1−4GlcNAcβ1-Asn-X-Ser/Thr [44] and are classified in three types: high-mannose, in which only mannose residues are attached to the core, like man5 and man9 used in the present study. Man5 is precursor of several high-mannose glycans, while man9 is found in a number of glycoproteins including insulin receptor and HIV gp120 [31,45,46], other potential therapeutical targets.

Complex type *N*-glycans, in which branches initiated by N-acetylglucosamine (GlcNAc) are attached to the core, being not uncommon the subsequent addition of galactose residues in β1−4

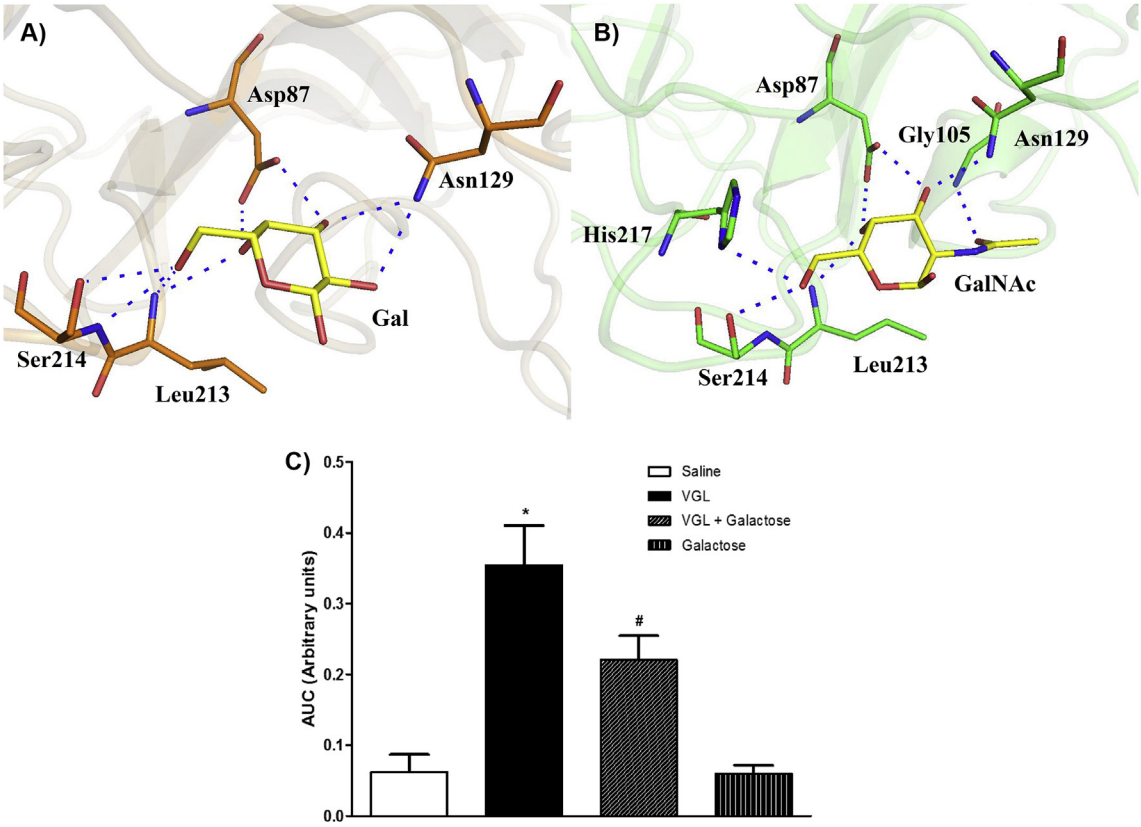

Fig. 6. CRD mediates VGL edematogenic effect. Representation of carbohydrate-recognition domain of VGL in complex with (a) D-galactose and (b) *N*-acetyl-D-galactosamine. Blue dashes represent polar contacts. (c) Inhibition of VGL-induced edema (1 mg/Kg; s.c.) by galactose (0.1 M). Mean ± S.E.M. (n = 5−6). *p < 0.05 *vs.* saline #p < 0.05 *vs.* VGL.

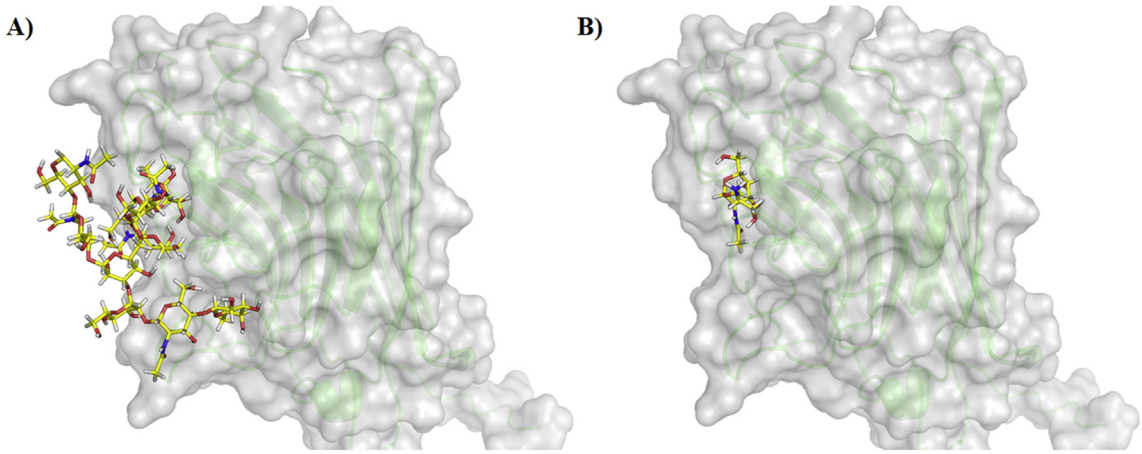

Fig. 7. Best docking poses of VGL complexed with A) CPLX1 glycan and B) Tn antigen.

bond with GlcNAc, named N-acetyllactosamine (LacNAc). Poly-LacNAc chains are found in glycans in various cell types and may serve as scaffold for insertion of specific glycosyl moieties [31]. Alternatively, formation of GalNAcβ 1–4GlcNAc branches are also present in several structures [47]. Complex glycan CPLX1 presents LacNAc and fucosylated GalNAcβ 1–4GlcNAc branches, while CPLX2 has similar structure to CPLX1 with LacNAc galactosyl terminal capped by a sialic acid.

Hybrid *N*-glycans have branches with unsubstituted mannose residues and others with GlcNAc linkage [48]. HBRD1 glycan presents the mannose residues branch and a sialic acid capped LacNAc branch, while HBRD2 have similar structure with uncapped galactosyl moiety.

Among *O*-glycans, docking revealed that, similar to VML [8,9], VGL possibly interacts with tumour-associated antigens T and Tn (Scores: −52.00 and −44.08), best pose of Tn antigen is shown in Fig. 7B, indicating a possible application in cancer research. Results also revealed very favorable interactions with *O*-glycans extended cores with exception of extended core 3.

O-glycans are important post-translational modification of mammalian proteins. Usually these glycans are linked via N-acetylgalactosamine (GalNAc) moiety to a serine or threonine residue [32]. Among the tested glycans, Tn antigen (GalNAcαSer/Thr) and T antigen (Galβ1-3GalNAcαSer/Thr) were chosen based on its importance in cancer studies and prevalence as cores of O-glycans [32,49,50]. Other chosen sugars include Excore1 that contains sialic acid capped LacNAc branch and are found in many glycoproteins and mucins, excore2 that contains a branching GlcNAc attached to core 1 and are found in both glycoproteins in specific cells and tissues, excore3 and excore4 that contains some LacNAc branches and are found in mucins of certain mucin-secreting tissues [51–53].

Most of biological activities triggered by lectins occur due to interaction between proteins and molecular targets via glycosyl residues [54–57] and together, these results suggest that VGL is capable of binding to *O*-glycans due to favorable docking scores and interactions suggestive of high specificity for this glycan type, while for N-glycans, the lectin binds to preferentially those possessing galactose as terminal residue. It is likely that the molecular target of VGL in order to elicit the edematogenic effect is a glycosylated protein presenting galactosyl moieties on its terminal regions or common types of *O*-glycans.

4. Conclusion

The theoretical three-dimensional structure of *Vatairea guianensis* lectin (VGL) presents high similarity with *Vatairea macrocarpa* lectin (VML). VGL elicited edematogenic activity, involving prostaglandins, IL-1β and CRD. *In silico* tests demonstrated the binding capacity of VGL with galactosides and important *N*- and *O*-glycans, corroborating with the hypothesis that VGL interaction with glycosylated molecular targets are one of the main factors responsible for its *in vivo* effects.

Conflict of interest

The authors declare that they have no conflict of interest.

Ethical approval

All procedures performed in animals were in accordance with the ethical standards of the institution at which the studies were conducted — UECE Institutional Ethical Committee (UECE No. 10130208-8/40).

This article does not contain any studies with human participants performed by any of the authors.

Acknowledgments

This study was supported by grants from the Conselho Nacional de Desenvolvimento Científico e Tecnológico (CNPq), Coordenação de Aperfeiçoamento de Pessoal de Nível Superior (CAPES) and Fundação Cearense de Apoio ao Desenvolvimento Científico e Tecnológico (FUNCAP). B.S.C., K.S.N., and A.M.S.A. are senior investigators of CNPq. David Martin helped with the English editing of the manuscript.

Appendix A. Supplementary data

Supplementary data related to this article can be found at http://dx.doi.org/10.1016/j.biochi.2017.06.008.

References

[1] H.S. Gabius, S. Gabius, Glycoscience: Status and Perspectives, WILEY-VCH Verlag, 1997.
[2] A.G. Rothfuchs, E. Roffe, A. Gibson, et al., Mannose-binding lectin regulates host resistance and pathology during experimental infection with *Trypanosoma cruzi*, Plos One 7 (11) (2012) e47835.
[3] B.S. Cavada, T. Barbosa, S. Arruda, et al., Revisiting proteus: do minor changes in lectin structure matter in biological activity? Lessons from and potential biotechnological uses of the Diocleinae subtribe lectins, Curr. Protein Pept. Sci. 2 (2) (2001) 123–135.

[4] A. Loris, A. Imberty, S. Beeckmans, et al., Crystal structure of *Pterocarpus angolensis* lectin in complex with glucose, sucrose, and turanose, J. Biol. Chem. 278 (18) (2003) 16297–16303.
[5] A.C. Almeida, V.J.S. Osterne, M.Q. Santiago, et al., Structural analysis of *Centrolobium tomentosum* seed lectin with inflammatory activity, Arch. Biochem. 15 (596) (2016) 73–83.
[6] R.G. Benevides, G. Ganne, R.C. Simões, et al., A lectin from *Platypodium elegans* with unusual specificity and affinity for asymmetric complex N-glycans, J. Biol. Chem. 287 (31) (2012) 26352–26364.
[7] R. Banerjee, S.V. Mande, V. Ganesh, et al., Crystal structure of peanut lectin, a protein with an unusual quaternary structure, Proc. Natl. Acad. Sci. 91 (1994) 227–231.
[8] B.L. Sousa, J.C. Silva-Filho, P. Kumar, et al., High-resolution structure of a new Tn antigen-binding lectin from *Vatairea macrocarpa* and a comparative analysis of Tn-binding legume lectins, Int. J. Biochem. Cell Biol. 59 (2015) 103–110.
[9] B.L. Sousa, J.C. Silva-Filho, P. Kumar, et al., Structural characterization of a *Vatairea macrocarpa* lectin in complex with a tumor-associated antigen: a new tool for cancer research, Int. J. Biochem. Cell Biol. 72 (2016) 27–39.
[10] N.M.N. Alencar, E.H. Teixeira, A.M.S. Assreuy, et al., Leguminous lectins as tools for studying the role of sugar residues in leukocyte recruitment, Mediat. Inflamm. 8 (2) (1999) 107–113.
[11] N.M.N. Alencar, C.F. Cavalcante, M.P. Vasconcelos, et al., Antiinflammatory and antimicrobial effect of lectin from *Lonchocarpus sericeus* seeds in an experimental model of infectious peritonitis, J. Pharm. Pharmacol. 57 (7) (2005) 919–922.
[12] M.H. Napimoga, B.S. Cavada, N.M. Alencar, et al., *Lonchocarpus sericeus* lectin decreases leukocyte migration and mechanical hypernociception by inhibiting cytokine and chemokines production, Int. Immunopharmacol. 7 (6) (2007) 824–835.
[13] A.F. Pires, N.V. Rodrigues, P.M. Soares, et al., A novel N-acetyl-glucosamine lectin of *Lonchocarpus araripensis* attenuates acute cellular inflammation in mice, Inflamm. Res. 65 (1) (2016) 43–52.
[14] N.M.N. Alencar, A.M.S. Assreuy, V.B. Alencar, et al., The galactose-binding lectin from *Vatairea macrocarpa* seeds induces *in vivo* neutrophil migration by indirect mechanism, Int. J. Biochem. Cell Biol. 35 (12) (2003) 1674–1681.
[15] N.M.N. Alencar, A.M.S. Assreuy, D.N. Criddle, et al., *Vatairea macrocarpa* lectin induces paw edema with leukocyte infiltration, Protein Pept. Lett. 11 (2) (2004) 195–200.
[16] N.M.N. Alencar, A.M.S. Assreuy, A. Havt, et al., *Vatairea macrocarpa* (Leguminosae) lectin activates cultured macrophages to release chemotactic mediators, Naunyn Schmiedeb. Arch. Pharmacol. 374 (4) (2007) 275–282.
[17] H.C. Silva, C.S. Nagano, L.A.G. Souza, et al., Purification and primary structure determination of a galactose-specific lectin from *Vatairea guianensis* Aublet seeds that exhibits vasorelaxant effect, Process Biochem. 47 (12) (2012) 2347–2355.
[18] E.C. Landucci, E. Antunes, J.L. Donato, et al., Inhibition of carrageenan - induced rat paw o edema by crotapotin, a polypeptide complexed with phospholipase A2, Br. J. Pharmacol. 114 (3) (1995) 578–583.
[19] R.F.G. Feitosa, G.B. Melcíades, A.M.S. Assreuy, et al., The pharmacological profile of ovalbumin-induced paw oedema in rats, Mediat. Inflamm. 11 (3) (2002) 155–163.
[20] M. Chaudhary, A.R. Gadbail, G. Vidhale, M.P. MankarGadbail, et al., Comparison of myofibroblasts expression in oral squamous cell carcinoma, verrucous carcinoma, high risk epithelial dysplasia, low risk epithelial dysplasia and normal oral mucosa, Head Neck Pathol. 6 (3) (2012) 305–313.
[21] D.W.A. Buchan, F. Minneci, T.C.O. Nugent, et al., Scalable web services for the PSIPRED protein analysis Workbench, Nucleic Acids Res. 41 (2013) 340–348.
[22] B. Webb, A. Sali, Comparative protein structure modeling using MODELLER, Curr. Protoc Protein Sci. 86 (2016), 2.9.1-2.9.37.
[23] R.A. Laskowski, M.W. MacArthur, D.S. Moss, et al., PROCHECK: a program to check the stereochemical quality of protein structures, J. Appl. Cryst. 26 (1993) 283–291.
[24] R. Lüthy, J.U. Bowie, D. Eisenberg, Assessment of protein models with three-dimensional profiles, Nature 356 (1992) 83–85.
[25] P. Benkert, M. Biasini, T. Schwede, Toward the estimation of the absolute quality of individual protein structure models, Bioinformatics 27 (2011) 343–350.
[26] P. Benkert, M. Kunzli, T. Schwede, QMEAN server for protein model quality estimation, Nucleic Acids Res. 37 (2009) 510–514.
[27] P. Benkert, S.C.E. Tosatto, D. Schomburg, QMEAN: a comprehensive scoring function for model quality assessment, Proteins 71 (2008) 261–277.
[28] The Pubchem Project https://pubchem.ncbi.nlm.nih.gov/, 2017 (Accessed 18 May 2017).
[29] O. Korb, T. Stützle, T.E. Exner, Empirical scoring functions for advanced protein-ligand docking with PLANTS, J. Chem. Inf. Model. 49 (2009) 84–96.
[30] A.C. Wallace, R.A. Laskowski, J.M. Thornton, LIGPLOT: a program to generate schematic diagram of protein-ligand interactions, Protein Eng. 8 (1995) 127–134.
[31] P. Stanley, H. Schachter, N. Taniguchi, Chapter 8: N-Glycans, in: A. Varki, R.D. Cummings, J.D. Esko, et al. (Eds.), Essentials of Glycobiology, second ed., Cold Spring Harbor, New York, 2009.
[32] I. Brockhausen, H. Schachter, P. Stanley, Chapter 9: O-GalNAc glycans, in: A. Varki, R.D. Cummings, J.D. Esko, et al. (Eds.), Essentials of Glycobiology, second ed., Cold Spring Harbor, New York, 2009.
[33] B.L. Parker, M. Thaysen-Andersen, N. Solis, et al., Site-specific glycan-peptide analysis for determination of N-glycoproteome heterogeneity, J. Proteome Res. 12 (12) (2013) 5791–5800.
[34] Glycan-Web, carbohydrate builder. http://glycam.org/tools/molecular-dynamics/oligosaccharide-builder/build-glycan?id=1, 2017 (Accessed 18 May 2017).
[35] D.A. Case, T.A. Darden, T.E. Cheatham, et al., AMBER 12, University of California, San Francisco, 2012.
[36] K.N. Kirschner, A.B. Yongye, S.M. Tschampel, et al., GLYCAM06: a generalizable biomolecular force field. Carbohydrates, J. Comput. 29 (4) (2008) 622–655.
[37] G. Jones, P. Willett, R.C. Glen, et al., Development and validation of a genetic algorithm for flexible docking, J. Mol. Biol. 267 (1997) 727–748.
[38] D. Salvemini, Z.Q. Wang, P.S. Wyatt, et al., Nitric oxide: a key mediator in the early and late phase of carrageenan-induced rat paw inflammation, Br. J. Pharmacol. 4 (1996) 829–838.
[39] S. Nikolaus, J. Bauditz, P. Gionchetti, et al., Increased secretion of pro-inflammatory cytokines by circulating polymorphonuclear neutrophils and regulation by interleukin 10 during intestinal inflammation, Gut 42 (1998) 470–476.
[40] A.M.S. Assreuy, M.D. Shibuya, G.J. Martins, et al., Anti-inflammatory effect of glucose-mannose binding lectins isolated from *Brazilian beans*, Mediat. Inflamm. 6 (1997) 201–210.
[41] K.V. Brinda, A. Surolia, S. Vishveshwara, Insights into the quaternary association of proteins through structure graphs: a case study of lectins, Biochem. J. 39 (2005) 1–15.
[42] T.K. Dam, B.S. Cavada, T.B. Grangeiro, et al., Diocleinae lectins are a group of proteins with conserved binding sites for the core trimannoside of asparagine-linked oligosaccharides and differential specificities for complex carbohydrates, J. Biol. Chem. 273 (1998) 12082–12088.
[43] R. Loris, F. Casset, J. Bouckaert, et al., The monosaccharide binding site of lentil lectin: an X-ray and molecular modelling study, Glycoconj. J. 11 (6) (1994) 507–517.
[44] S.S. Pinho, C.A. Reis, Glycosylation in cancer: mechanisms and clinical implications, Nat. Rev. Cancer 15 (9) (2015) 540–555.
[45] A.P. Cornfield, Structure/function of O-glycans. In: encyclopedia of genetics, genomics, Proteomics Bioinformatics 3 (3) (2005), 5:65.
[46] J. Mitoma, B. Petryniak, N. Hiraoka, et al., Extended core 1 and core 2 branched O-glycans differentially modulate sialyl Lewis X-type L-selectin ligand activity, J. Biol. Chem. 278 (11) (2003) 9953–9961.
[47] A. Guzman-Aranquez, P. Arqueso, Structure and biological roles of mucin-type O-glycans at the ocular surface, Ocul. Surf. 8 (1) (2010) 8–17.
[48] V.R. Pinto-Junior, M.Q. Osterne VJS Santiago, et al., Structural studies of a vasorelaxant lectin from *Dioclea reflexa* hook seeds: crystal structure, molecular docking and dynamics, Int. J. Biol. Macromol. 98 (2017) 12–23.
[49] H. Yao, X. Xie, Y. Li, Legume lectin FRIL preserves neural progenitor cells in suspension culture in vitro, Clin. Dev. Immunol. 2008 (2008) 531317.
[50] D.O. Croci, J.P. Cerliani, T. Dalotto-Moreno, et al., Glycosylation-dependent lectin-receptor interactions preserve angiogenesis in anti-VEGF refractory tumors, Cell 156 (4) (2014) 744–758.
[51] G.A. Bezerra, R. Viertlmayr, T.R. Moura, et al., Structural studies of an anti-inflammatory lectin from *Canavalia boliviana* seeds in complex with dimannosides, PLoS One 9 (5) (2014) e97015.
[52] E. Bieberich, Synthesis, processing, and function of N-glycans in N-glycoproteins, Adv. Neurobiol. 9 (2015) 47–70.
[53] L.G. Sparrow, M.C. Lawrence, J.J. Gorman, et al., N-linked glycans of the human insulin receptor and their distribution over the crystal structure, Proteins 71 (1) (2008) 426–439.
[54] S. Sirois, M. Touaibia, K.C. Chou, et al., Glycosylation of HIV-1 gp120 V3 loop: towards the rational design of a synthetic carbohydrate vaccine, Curr. Med. Chem. 14 (30) (2007) 3332–3342.
[55] D.H. Van den Eijnden, A.P. Neeleman, H. Bakker, et al., Novel pathways in complex-type oligosaccharide synthesis. New vistas opened by studies in invertebrates, Adv. Exp. Med. Biol. 435 (1998) 3–7.
[56] B. Schiller, A. Hykollari, S. Yan, Complicated N-linked glycans in simple organisms, Biol. Chem. 393 (8) (2012) 661–673.
[57] K. Mariño, J. Bones, J.J. Kattla, et al., A systematic approach to protein glycosylation analysis: a path through the maze, Nat. Chem. Biol. 6 (10) (2010) 713–723.